

Gold Nanoparticles Modified Electrode for the Determination of an Antihypertensive Drug

Nada F. Atta,* Ahmed Galal, Shereen M. Azab

Department of Chemistry, Faculty of Science, Cairo University, Postal Code, 12613 Giza, Egypt

tel: +0237825266; fax: +0235727556

*e-mail: nada_fah1@yahoo.com; galal@sci.cu.edu.eg

Received: March 29, 2012

Accepted: April 2, 2012

Abstract

The nature of binding between Terazosin (TR) and gold nanoparticles (Au-Nps) is investigated using UV-vis and fluorescence spectroscopies, cyclic voltammetry, SEM, and EIS. The results suggest that Au-Nps are effective carriers for TR. An electrochemical sensor for TR is introduced using Au-Nps electrodeposited on carbon paste electrode. The effect of parameters including pH and scan rate on the response was investigated. A linear range from 8.0×10^{-9} to $5.4 \times 10^{-5} \text{ mol L}^{-1}$ with correlation coefficient of 0.9995 and detection limit of $1.2 \times 10^{-10} \text{ mol L}^{-1}$ was obtained. This sensor was used for determining TR spiked in urine, and excellent recovery results are achieved.

Keywords: Terazosin, Gold nanoparticles, Electrochemical sensor, Impedance spectroscopy

DOI: 10.1002/elan.201200169

Supporting Information for this article is available on the WWW under <http://dx.doi.org/10.1002/elan.201200169>.

1 Introduction

Terazosin hydrochloride (TR): 2-[4-(2-tetrahydrofuranyl carbonyl)-1-piperazinyl-6,7-dimethoxy-4-quinazolinamine monohydro-chloride hydrate is classified as a quinazolinone (Scheme 1).

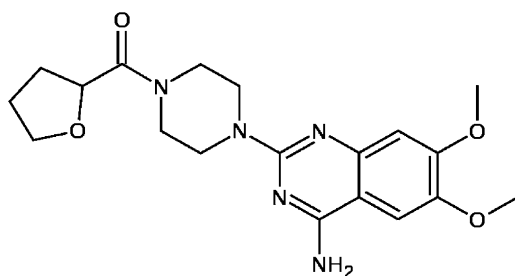
It is a highly selective adreno-receptor antagonist, an effective drug for hypertension [1,2] by relaxing veins and arteries, and for the symptomatic treatment of urinary obstruction caused by benign prostatic hyperplasia (BPH) by relaxing the muscles of the bladder and prostate [3–6]. TR is rapidly and almost completely adsorbed from the gastro-intestinal tract after oral administration. The reported bioavailability is about 90%. It undergoes extensive hepatic metabolism, and the major route of elimination is via the biliary tract. Different analytical methods have been reported for determination of Terazosin in bulk form, pharmaceuticals and biological fluids following intravenous and oral dosage. These include spectropho-

tometry [7–10], spectrofluorimetry [10–13], HPLC[14], voltammetry [15,16] HPLC with UV detection [17,18], and with fluorescence detection [18–20], normal phase HPLC electrospray mass spectroscopy [21] and HPLC with photodiode array detection [22].

Electrochemical methods have proved to be sensitive, accurate and reliable for the determination of organic molecules that undergo oxidation or reduction reactions, and plays important role in drug quality control and related molecules in pharmaceutical dosage forms and biological fluids [23–28]. Therefore, the development of sensitive, simple, rapid and reliable method for the determination of active ingredient in drugs is of great importance and interest.

Carbon paste electrodes are currently widespread use in electroanalytical chemistry, because of their broad potential window, low cost, rich surface chemistry, low background current and chemical inertness. Carbon paste electrode (CPE) has some special characteristics and benefits such as the ease of surface renewal, individual polarizability and easy to apply modifications.

Electrodeposition of gold nanoparticles onto the surface of the CP-electrode was another strategy to enhance the sensitivity of the immunosensor. Several research work had been conducted to construct CP-electrode modified with gold nanoparticles to be used as an immunosensor for the determination of α -fetoprotein [29], carcinoma antigen [30], or in streptavidin-biotin interaction [31], or as an enzyme biosensors [32]. Electrodeposition of gold nanoparticles onto other surfaces as, glassy carbon [33,34], monitoring of silver and gold electrode-



Scheme 1. Terazosin.

position on glassy carbon and silicon [35], screen-printed [36] and indium/tin oxide surfaces [37–42] were also studied.

In this work, we introduce a highly sensitive gold/carbon-paste composite electrode for the sensitive detection of TR in the presence of interferents in human urine and in pharmaceutical formulations. Furthermore, gold nanoparticles have the potential to be used as effective carriers for TR drugs. This should result in enhancing the drug bioavailability and protection of drug bioactivity and stability. Thus, sensitive electrochemical detection of TR using carbon paste electrodes modified with gold nanoparticles will be demonstrated. Complex formation and binding interactions between TR and gold nanoparticles using UV-vis and fluorescence spectroscopies, and electrochemical impedance is also explored.

2 Experimental

2.1 Materials and Reagents

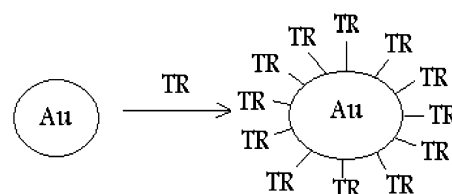
Terazosin hydrochloride and Itrin tablets (2.0 mg per tablet) were supplied by Kahira Pharmaceutical and Chemical Industries Co. (Egypt). A stock solution of TR ($1.0 \times 10^{-3} \text{ mol L}^{-1}$) was prepared with deionized water. Diluted working standard solutions were then prepared daily with deionized water freshly just prior to use. Britton–Robinson (B–R) ($\text{CH}_3\text{COOH} + \text{H}_3\text{BO}_3 + \text{H}_3\text{PO}_4$) ($4.0 \times 10^{-2} \text{ mol L}^{-1}$) buffer solution of pH 2–11 was used as the supporting electrolyte. The pH was adjusted using 0.2 M NaOH. All solutions were prepared from analytical grade chemicals and sterilized Milli-Q deionized water.

2.1.2 Preparation of Citrate Capped Gold Nanoparticles

Trisodium citrate (38.8 mM, 50 mL) was added to a boiling HAuCl_4 solution (1 mM, 500 mL). After the addition, the previously yellow solution of gold chloride turned wine red in color and gave a characteristic absorbance at 518 nm in the UV-vis spectrum [43].

2.1.3 Preparation of TR Coated Gold Nanoparticles

Citrate-stabilized gold nanoparticles (1 mM, 50 mL) were mixed with TR (5 mM) in H_2O (25 mL) and stirred effectively until the wine red color became blue. The UV-vis spectrum was obtained after mixing TR with gold nanoparticles. The reaction scheme is given in Scheme 2. Due to the good correlation between the drug's coordination (it contains oxygen and nitrogen) donor sites for binding with gold nanoparticles. Thus, Scheme 2 shows a schematic diagram that elucidates the aggregation of TR on gold nanoparticles [43,44].



Scheme 2. Aggregation of TR on gold nanoparticles.

2.1.4 Construction of Gold Nanoparticles Modified CP-Electrode (GNMCPE)

The CP-electrode was fabricated as described elsewhere [45] then was immersed into 6 mM hydrogen-tetrachloroaurate HAuCl_4 solution containing 0.1 M KNO_3 (prepared in doubly distilled water, and deaerated by bubbling with nitrogen). A constant potential of -0.4 V versus Ag/AgCl was applied for 400 s. Then, the modified electrode (GNMCPE) was washed with doubly distilled water and dried carefully.

2.2 Instrumental and Experimental Set-up

2.2.1 UV Study

All UV measurements were performed using a Shimadzu 1601 spectrophotometer (Kyoto, Japan). The path length was 1 cm and matched 1 cm \times 1 cm cuvettes were used. Spectrofluorimetric measurement was carried out using a Shimadzu spectrofluorimeter Model RF-1501 equipped with xenon lamp and 1-cm glass cells. Excitation wavelength was set at 336 nm.

2.2.2 Electrochemical Measurements

All voltammetric measurements were performed using a PC-controlled AEW2 electrochemistry work station and data were analyzed with ECprog3 electrochemistry software, manufactured by Sycopel Scientific Ltd (Tyne & Wear, UK). The one compartment cell with the three electrodes was connected to the electrochemical workstation through a C3-stand from BAS (USA). A platinum wire from BAS (USA) was employed as auxiliary electrode. All the cell potentials were measured with respect to Ag/AgCl (3 M NaCl) reference electrode from BAS (USA). One compartment glass cell (15 mL) fitted with gas bubbler was used for electrochemical measurements. Solutions were degassed using pure nitrogen prior and throughout the electrochemical measurements. A Jenway 3510 pH meter (England) with glass combination electrode was used for pH measurements. Scanning electron microscopy (SEM) measurements were carried out using a JSM-6700F scanning electron microscope (Japan Electro Company). All the electrochemical experiments were performed at an ambient temperature of $25 \pm 2^\circ\text{C}$.

2.2.3 Impedance Spectroscopy Measurements

Electrochemical impedance spectroscopy was performed using a Gamry-750 system and a lock-in-amplifier that are connected to a personal computer. The data analysis software was provided with the instrument and applied nonlinear least square fitting with Levenberg-Marquardt algorithm. All impedance experiments were recorded between 0.1 Hz and 100 kHz with an excitation signal of 10 mV amplitude.

2.3 Itrin Tablet Solutions

Five Itrin tablets (2 or 5 mg) were weighed and the average mass per tablet was determined. A portion of the finely ground Terazosin was accurately weighed and transferred into a 100-mL volume calibrated flask. The flask was sonicated for about 15 min and then made up to the volume with B–R buffer. The solution was then filtered to separate out the insoluble excipients, rejecting the first portion of the filtrate. The desired concentrations of the drug were obtained by accurate dilution with B–R buffer and used as standard solutions. An aliquot volume of the solution was transferred into a 10-mL volume calibrated flask then made up to the volume with the supporting electrolyte. The solution was directly analyzed, according to the general analytical procedure without the necessity for sample pretreatment or any extraction steps.

2.4 Analysis of Urine

Standard TR provided by the National Organization for Drug Control and Research of Egypt was dissolved in urine to make a stock solution with $1.0 \times 10^{-3} \text{ mol L}^{-1}$ concentration. Successive additions of TR $1.0 \times 10^{-3} \text{ M}$ in urine were added to 5 mL B–R buffer pH 7.4.

3 Results and Discussion

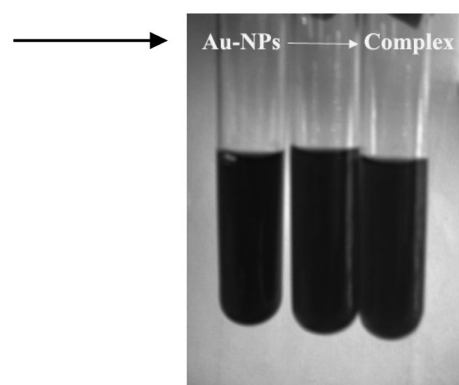
3.1 Spectral Study

3.1.1 Interaction of Gold Nanoparticles with TR

Interactions of Au-Nps with TR in aqueous B–R buffer solutions pH 7.4 were followed by UV-vis spectroscopy. The plasmon band observed for (0.5 mM) wine red colloidal gold at 520 nm in the UV-vis spectrum is characteristic of gold nanoparticles. 0.15 mM TR shows a maximum at 321 nm (Supporting Information 1).

The Au-Nps exhibit strong surface plasmon resonance (SPR) absorption that is dependent on the size and shape of particles. For spherical Au-Nps, the SPR band maximum generally falls between about 520 and 530 nm [47].

By continuous addition of colloidal gold to pure TR, both the bands at 321 and 520 nm pertaining to pure drug and Au colloids decrease in intensity steadily. This decrease is accompanied by emergence of an additional peak at 640 nm (Figure 1): i.e. a change from wine red to



Photograph 1. Change from wine red to violet to blue with the addition of drug to colloidal gold.

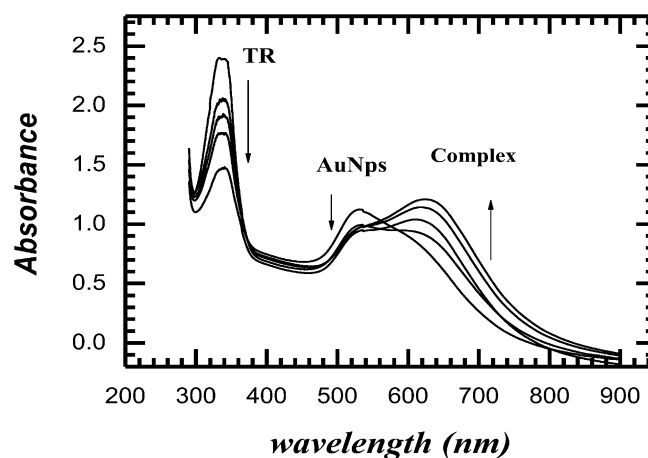


Fig. 1. Time-dependent UV-vis spectrum obtained after mixing 0.15 mM TR to 0.5 mM gold nanoparticles at a timed interval of 5 min.

violet to blue with the addition of drug to colloidal gold (Photograph 1). The appearance of the new peak is due to the aggregation of gold nanoparticles and the replacement of citrate by TR leading to the formation of gold–drug complex. This reaction provides an important means for the chemical functionalization of the nanoparticles and greatly extends the versatility of these systems [47].

3.1.2 Optical Properties of Drugs Coated Gold Nanoparticles

In this experiment we will study the stoichiometric ratio of the complex formation for the drug and gold nanoparticles (Au-Nps) by applying molar ratio [48] (Supplement 2A) and continuous variation methods (cvm) [49] (Supporting Information 2B). The molar ratio method is used to know the number of moles of a particular reactant needed to completely react with a certain number of moles of a second reactant, so, a constant concentration of Au-Nps (0.1 mM) was added to different concentrations (0.05–0.3 mM) of TR drug in 5 mL B–R buffers

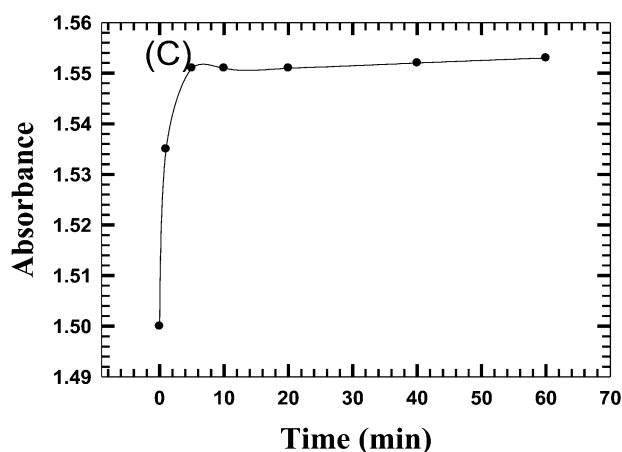


Fig. 2. Effect of time on complex stability studied for 60 minutes.

(pH 7.4). The absorbance of each solution was measured and plotted against the drug concentration and it was found that the maximum absorbance occurred after the addition of 0.15 mM TR. While continuous variation method is performed by preparing several solutions consisting of varying amounts of the drug and (Au-Nps), however the sum of the drug concentration and gold concentration is constant for each solution. The absorbance of each solution is measured and plotted against the mole fraction of drug or mole fraction of Au-Nps. The mole fraction of the drug, d , is defined as:

$$\text{mole fraction} = C_d / (C_d + C_{Au})$$

where C_d is the concentration of the drug and C_{Au} is the concentration of Au-Nps.

Therefore, the absorbance data obtained were plotted against the mole fraction of the drug, and the result shows that the maximum absorbance was found when the mole fraction was 0.2 which means that the complex is 1:4, i.e. 1 mol of TR needs 4 mol of Au-Nps to form a complex which gives the maximum absorbance. Also the effect of time on the stability of the complex (1:4) was studied for 60 minutes (Figure 2), as can be seen the absorbance increased slightly and then became stable after 5 minutes.

3.2 Binding Interaction from Fluorescence Studies

Fluorescence studies offer an excellent probe for confirming the binding of drug with gold nanoparticles as it has been previously reported that gold metal efficiently quenches the emission of many fluorophores [50–52]. In the present investigation, 0.2×10^{-3} M TR was initially highly fluorescent but with the addition of gold colloids, quenching of fluorescence was observed. Gold nanoparticles are non-fluorescent while pure TR showed a high and a broad emission centered at around 380 nm when

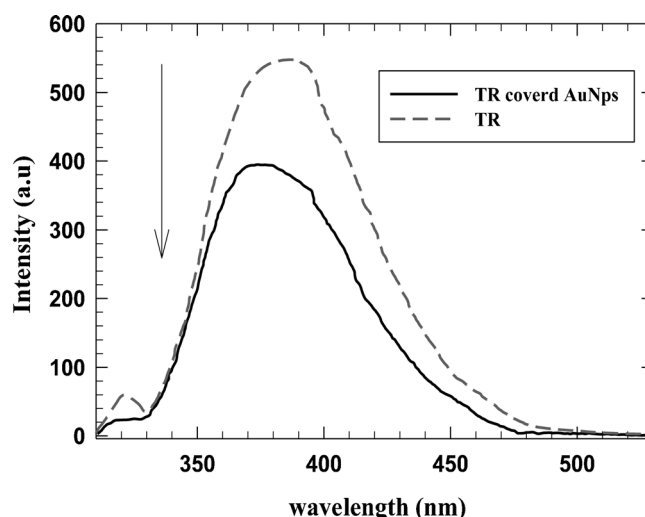


Fig. 3. Emission spectra of (0.2 mM) TR (---) and (2) TR covered gold nanoparticles (—) taken in aqueous medium.

excited at a wavelength of 336 nm; in the presence of gold nanoparticles, the fluorescence intensity was reduced and this quenching of intensity can be attributed to the electronic interactions between the drug molecule and gold nanoparticles (Figure 3). Owing to the binding of TR on the surfaces of the gold nanoparticles, the electronic environment is altered thus resulting in quenching of fluorescence.

3.3 Electrochemistry of TR at GNMCPPE

To support the binding of TR moiety on gold nanoparticles, cyclic voltammetry was employed; GNMCPPE was used as working electrode. The voltammetric behavior of TR was examined. Figure 4 shows typical cyclic voltammograms of 1.0×10^{-3} mol L⁻¹ of TR in B–R buffer pH 7.4 at scan rate 100 mV s⁻¹ recorded at two different working electrodes (i.e. a bare CP (solid line) and GNMCPPE (dashed lines) electrodes, respectively).

As can be seen from Figure 4, The voltammograms exhibited a single well-defined two electron irreversible oxidation peaks, at GNMCPPE the oxidation peak current was 174 μ A, i.e., higher compared to that of bare CP-electrode which was 38 μ A, this is due to the larger real surface area of the modified electrode. The electrodeposition of Au particles on CP-electrode resulted in an observable increase in the peak current, which indicated an improvement in the electrode kinetics. The results confirmed the key role played by Au-Nps on the catalytic oxidation which enhances the electrochemical reaction. At this pH TR is protonated and gold nanoparticles are negatively charged and that is how the attraction takes place.

3.4 Morphologies of the Different Electrodes

The response of an electrochemical sensor was related to its physical morphology. The SEM of CP-electrode and

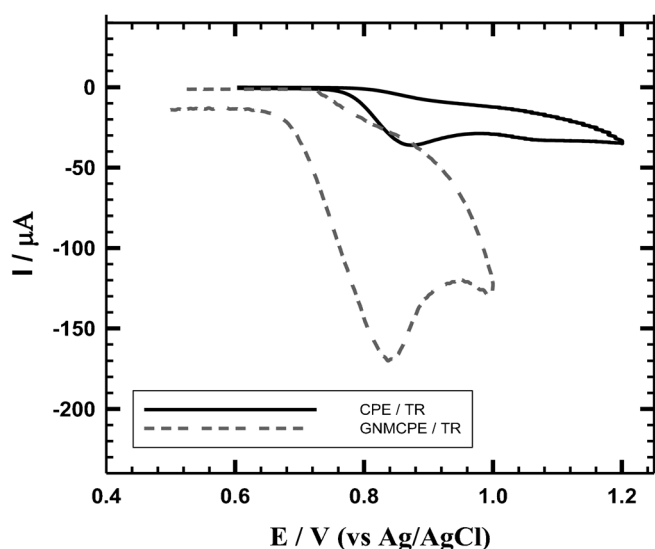


Fig. 4. Cyclic voltammograms of $1.0 \times 10^{-3} \text{ mol L}^{-1}$ TR in B-R buffer pH 7 at scan rate 100 mV s^{-1} recorded at two different working electrodes 1) bare CPE (—) and 2) GNMCPPE (----).

GNMCPPE were shown in Figure 5. Significant differences in the surface structure of CP-electrode and GNMCPPE were observed. The surface of the CP-electrode was predominated by isolated and irregularly shaped graphite flakes and separated layers were noticed (Figure 5A). The SEM image of GNMCPPE (Figure 5B) shows that metallic nanoparticles are located at different elevations over the substrate. Moreover, a random distribution and interstices among the nanoparticles were observed in the SEM image of the GNMCPPE exhibiting large surface area.

3.5 Effect of Operational Parameters

3.5.1 Effect of Solution pH

The effect of solution pH on the electrocatalytic oxidation of TR at the GNMCPPE was studied by cyclic voltammogram technique using Britton–Robinson buffers within the pH range of 2–11. As shown in Figure 6, the peak current intensities recorded at different pH values show that much higher peak current intensity was achieved in B–R

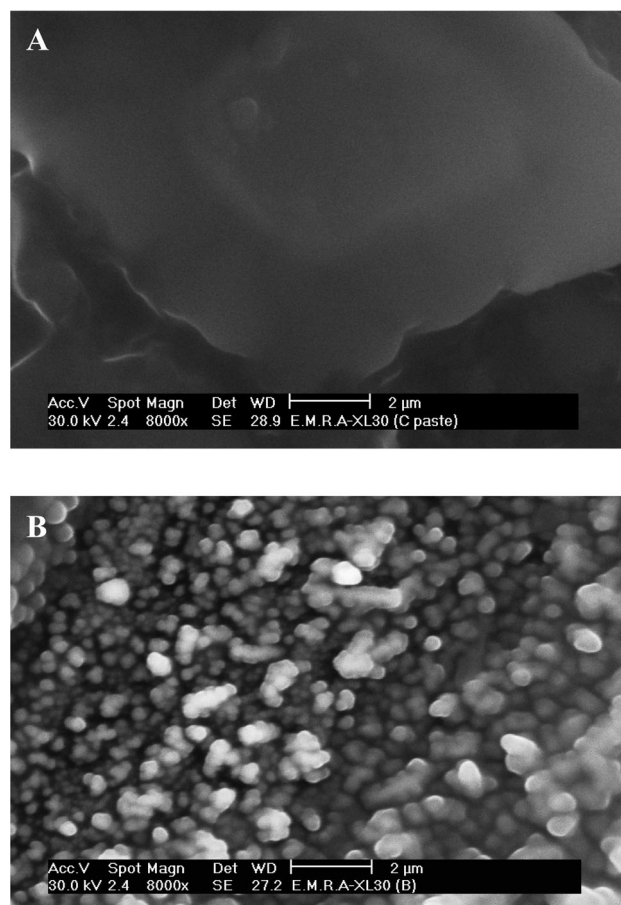
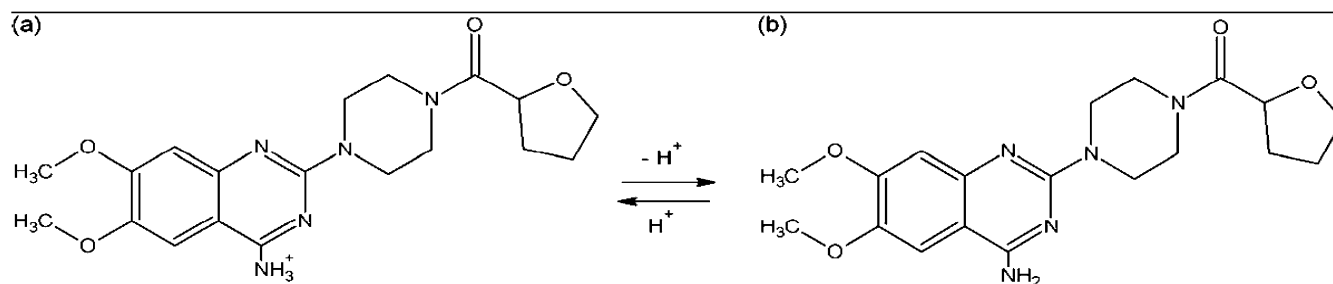


Fig. 5. Scanning electron microscope image of A) bare CPE and B) GNMCPPE.

buffers of pH 7. This behavior may be attributed acid–base equilibrium involved at working pH, whereas protonated aromatic amine group (a) of TR which acts as a weak base was converted to its dissociated form (b) (Scheme 3) due to the $\text{p}K_{\text{a}}$ of TR which is 7.1 [53]. Therefore, B–R buffer of pH 7.4 which is the body physiological pH value was used as a supporting electrolyte in the rest of the present work.

From Figure 6 Inset A, it was found that the pH of the solution has a significant influence on the catalytic oxidation of TR, indicating that the electrocatalytic oxidation at the GNMCPPE is a pH-dependent reaction. Also, from



Scheme 3. Acid–base equilibrium involved at working pH, whereas protonated aromatic amine group (a) of TR which acts as a weak base was converted to its dissociated form (b).

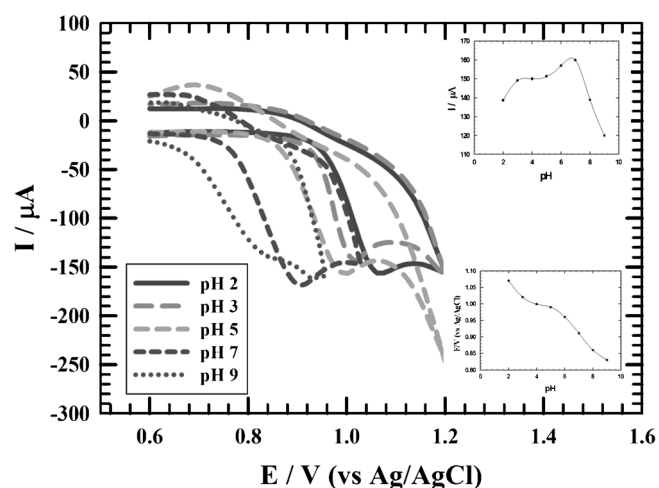


Fig. 6. Cyclic voltammogram of the effect of solution pH on the electrocatalytic oxidation of TR at GNMCPe using Britton–Robinson buffers within the pH range of 2–9. Inset 1: Plot of the anodic peak current values versus pH. Inset 2: Plot of the anodic peak potential values versus pH.

Figure 6 Inset B it was found that the peak potential for TR oxidation shifts to negative values linearly with the increase of pH of the medium (over the pH range from 2 to 11), denoting that protons are involved in the electrode reaction process and that the proton-transfer reaction proper precedes the electrode process [54]. The dependence of E_{pa} on the pH at the GNMCPe can be expressed by the equation E_{pa} (V) = 1.122 – 0.032 pH vs. Ag/AgCl with a correlation coefficient of 0.994. As TR oxidation is known to involve two protons and two electrons, the slope would be expected to be 59 mV pH⁻¹. The 32 mV pH⁻¹ slope obtained in the present studies indicates that the electrode process is more complex.

3.5.2 Influence of the Scan Rate

The effect of different scan rates (ν ranging from 10 to 250 mV s⁻¹) on the current response of TR (1.0×10^{-3} mol L⁻¹) on GNMCPe in B–R buffer (pH 7.4) was studied and the plot of i_{pa} versus $\nu^{1/2}$ gave a straight line. This revealed that the linearity of the relationship was realized up to a scan rate of 100 mV s⁻¹ followed by a deviation from linearity with further increase of the scan rate. This indicated that the charge transfer was under diffusion control. Typical CV curves of TR at different scan rates were shown in Supporting Information 3. A good linear relationship was found for the oxidation peak currents and potentials, with different scan rates (Supporting Information 3 Insets). The oxidation peak currents increased linearly with the linear regression equations as i_{pa} (10^{-6} A) = 17.394 $\nu^{1/2}$ (V s⁻¹)^{1/2} – 25.386 ($n=5$, $\gamma=0.9941$) suggesting that the reaction is a diffusion-controlled electrode reaction.

3.5.3 Diffusion Coefficients of TR

The dependence of the anodic peak current density on the scan rate has been used for the estimation of the “apparent” diffusion coefficient, D_{app} , for the compounds studied. D_{app} values were calculated from Randles–Sevcik equation [28], and for the oxidized species [O]:

$$I_p = 0.4463 (F^3/RT)^{1/2} n^{3/2} \nu^{1/2} D_0^{1/2} A C_0$$

For $T=298$ K (temperature at which the experiments were conducted), the equality holds true:

$$i_{pa} = (2.69 \times 10^5) n^{3/2} A C_0^* D_0^{1/2} \nu^{1/2}$$

Where the constant has unit (i.e. 2.687×10^5 C mol⁻¹ V^{-1/2}).

In these equations: I_p is the peak current density (A cm⁻²), n is the number of electrons appearing in the half-reaction for the redox couple, ν is the rate at which the potential is swept (V s⁻¹), F is Faraday’s constant (96485 C mol⁻¹), C_0 is the analyte concentration (1×10^{-6} mol L), A is the electrode area (0.0706 cm²), R is the universal gas constant (8.314 J mol⁻¹ K⁻¹), T is the absolute temperature (K), and D is the electroactive species diffusion coefficient (cm² s⁻¹). Apparent surface area used in the calculations did not take into account the surface roughness.

The apparent diffusion coefficients, D_{app} , of TR on GNMCPe and bare CP-electrode in B–R buffer (pH 7.4) were calculated from cyclic voltammetry (CV) experiments and was found to be 7.09×10^{-5} cm² s⁻¹ and 4.20×10^{-6} cm² s⁻¹ respectively, indicating a quick mass transfer of the analyte molecules towards GNMCPe surface from bulk solutions and/or fast electron transfer process of electrochemical oxidation of the analyte molecule at the electrode-solution interface [55,56]. Furthermore, it also showed that the oxidation reaction of the analyte species takes place at the surface of the electrode under the control of the diffusion of the molecules from solution to the electrode surface. The calculated D_{app} values at bare CP-electrode and GNMCPe showed that Au particles improve the electron transfer kinetics at the electrode/solution interface.

3.6 Electrochemical Impedance Spectroscopy (EIS) Studies

EIS is an effective tool for studying the interface properties of surface-modified electrodes. EIS data were obtained for GNMCPe at AC frequency varying between 0.1 Hz and 100 kHz with an applied potential in the region that corresponds to the electrolytic oxidation of TR in B–R buffer pH 7.4. Figure 7 shows a typical impedance spectrum presented in the form of Nyquist plot of TR using bare CP-electrode (A) and GNMCPe (B) at the oxidation potential 820 mV and a simple equivalent circuit model in Figure 7C was used to fit the results. From this comparison, it is clear that the impedance re-

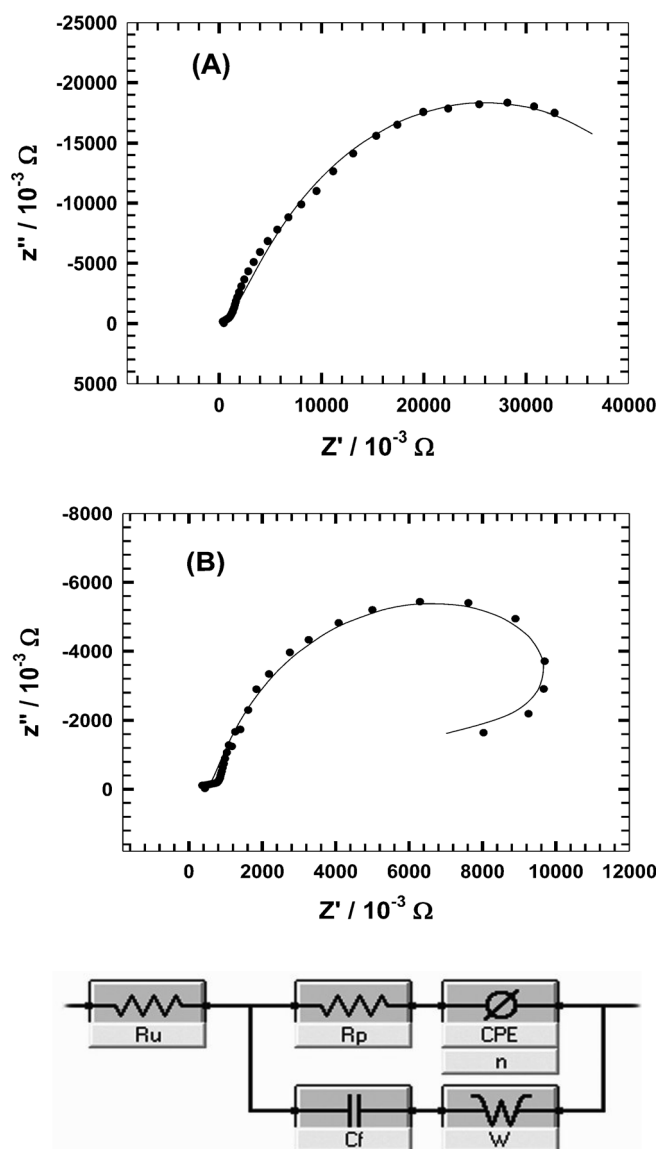


Fig. 7. A) Typical impedance spectrum presented in the form of Nyquist plot of TR using bare CP electrode at the oxidation potential 820 mV. (Symbols and solid lines represent the experimental measurements and the computer fitting of impedance spectra, respectively). B) The typical impedance spectrum presented in the form of Nyquist plot of TR using GNMCP electrode at the oxidation potential 820 mV. (Symbols and solid lines represent the experimental measurements and the computer fitting of impedance spectra, respectively). C) Equivalent circuit used in the fit procedure of the impedance spectra.

sponses of TR show great difference in the presence of gold nanoparticles. In case of using bare CP electrode,

the impedance spectra of TR response include a semi-circle with a larger diameter compared to GNMCP electrode. After deposition of gold, the diameter of the semi-circle diminishes markedly. This indicates that the charge transfer resistance of electrooxidation of TR decreases and response is enhanced. The equivalent circuit of Figure 7C was used to fit the results.

The experimental data were compared with an “equivalent circuit”. In this circuit, R_u is the solution resistance, R_p is the polarization resistance, CPE represents the predominant diffusion influence on the charge transfer process, n is its corresponding exponent. C_f is the capacitance of the double layer and W is the Warburg impedance due to diffusion. Table 1 lists the best fitting values calculated from the equivalent circuit for the impedance data. From the data indicated in Table 1, the value of solution resistance, R_u , was almost constant within the limits of the experimental errors. On the other hand, CPE shows noticeable increase in values in case of GNMCP electrode compared to CP-electrode which indicates less electronic resistance and more facilitation of charge transfer. This is explained in terms of the increase in the ionic adsorption at the electrode/electrolyte interface. Moreover, the decrease in the interfacial electron transfer resistance is attributed to the selective interaction between gold nanoparticles and TR that resulted in the observed increase in the current signal for the electrooxidation process.

3.7 General Procedure for the Determination of TR in the Pure Form

The GNMCP electrode was immersed in 5 mL of B–R buffer solution of pH 7.4. Aliquots of the drug solution ($1.0 \times 10^{-3} \text{ mol L}^{-1}$) were introduced into the electrolytic cell and voltammetric analyses were carried out and the voltammograms were recorded. The peak current was evaluated as the difference between each voltammogram and the background electrolyte voltammogram. All measurements were carried out at the room temperature.

To prove the sensitivity of the GNMCP electrode towards the electrochemical measurement of TR, the effect of changing the concentration of TR in B–R buffer pH 7.4, using differential pulse mode (DPV) (Figure 8). The following are the parameters for the DPV experiments: $E_i = +500 \text{ mV}$, $E_t = +1000 \text{ mV}$, scan rate = 10 mV s^{-1} , pulse width = 25 ms, pulse period = 200 ms, and pulse amplitude = 10 mV. The corresponding calibration plot was given in the inset. The calibration plot (Figure 8 Inset) was linearly related to TR concentration over the range of 8.0×10^{-9} to $5.4 \times 10^{-5} \text{ mol L}^{-1}$ with the regression equation

Table 1. Electrochemical impedance spectroscopy fitting data corresponding to Figure 8.

Electrode	E (mV)	R_p ($\text{k}\Omega \text{ cm}^2$)	R_u ($\text{k}\Omega \text{ cm}^2$)	C_f ($\mu\text{F cm}^{-2}$)	W ($\text{k}\Omega^{-1} \text{ cm}^{-2}$)	CPE ($\mu\text{F cm}^{-2}$)	n
Bare CPE	820	46.17	0.49	7.36	30.81	22.65	0.69
GNMCP	820	12.55	0.46	29.60	3.99	52.64	0.7

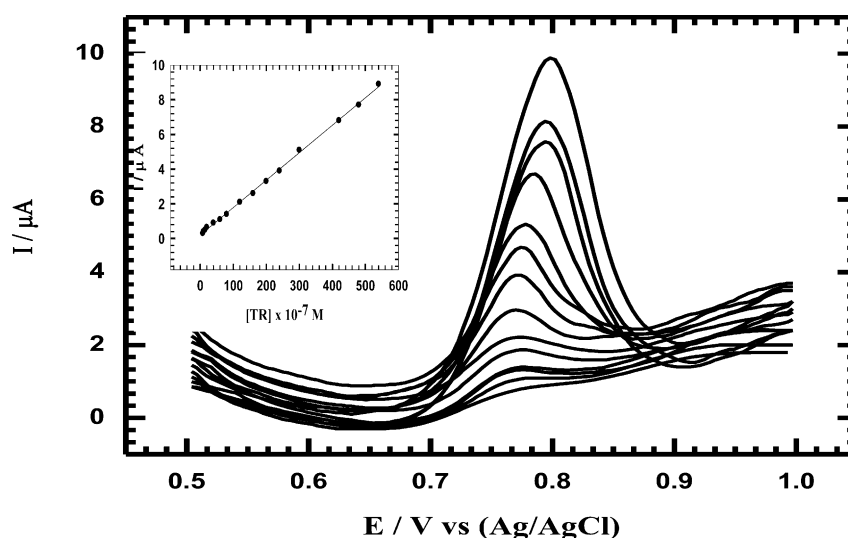


Fig. 8. Effect of changing the concentration of TR, using differential pulse mode at GNMCPe in 0.04 M B–R buffer pH 7.4 and a scan rate of 10 mV/s. Inset: Relation between TR concentration and current responses.

Table 2. Recovery data obtained by standard addition method for (TR) in drug formulation.

Formulation	[Tablet] taken $\times 10^{-5}$ M	[Standard] added $\times 10^{-5}$ M	Found $\times 10^{-6}$ M	Recovery (%)	RSD (%)
Itrin	1.00	2.0	3.03	101.0	0.32
	8.00		10.04	100.4	0.43
	20.0		21.80	99.10	0.33
	48.0		50.32	100.6	0.54

tion of $I_p(\mu\text{A}) = 0.0158 c(\mu\text{M}) + 0.202$ and the correlation coefficient was 0.9995. The limit of detection (LOD) and the limit of quantitation (LOQ) were calculated from the oxidation peak currents of the linear range using the following equations [57]:

$$LOD = 3 s/m$$

$$LOQ = 10 s/m$$

Where s is the standard deviation of the oxidation peak currents (three runs) and m is the slope ($\mu\text{A M}^{-1}$) of the related calibration curves, and they were found to be $1.2 \times 10^{-10} \text{ mol L}^{-1}$ and $4.14 \times 10^{-10} \text{ mol L}^{-1}$ respectively. Both LOD and LOQ values confirmed the sensitivity of GNMCPe.

3.8 Analytical Application

3.8.1 Analysis of Itrin Tablets

The determination of TR in its pharmaceutical formulation (5 mg/tablet) without the necessity for any extraction steps was performed.

Five tablets of Itrin were weighed and the average mass per tablet was determined, then these tablets were powdered. A portion of the fine powder needed to obtain $1.0 \times 10^{-3} \text{ mol L}^{-1}$. Aliquots of the drug solution were introduced into the electrolytic cell and the general procedure

was carried out based on the average of three replicate measurements. The average standard TR concentration was taken as a base value. Then, known quantities of Itrin were added to the aliquot, and its concentrations were determined following the developed procedure. From Table 2 we can see that the recovery data obtained by the standard addition method for TR in drug formulation was found in the range from 99.1% to 101.0% and the relative standard deviation (RSD) was in the range from 0.32% to 0.54% suggesting that GNMCPe has higher reproducibility and that there were no important matrix interferences for the samples analyzed by DPV mode. It would be a useful electrode for quantitative analysis of TR in pharmaceutical formulations.

3.8.2 Validation Method in Urine

Validation of the procedure for the quantitative assay of TR was examined in B–R buffer pH 7.4, at a scan rate of 10 mV/s using DPV. The calibration curve (Figure 9) gave a straight line in the linear dynamic range of $2 \times 10^{-7} \text{ mol L}^{-1}$ – $3 \times 10^{-5} \text{ mol L}^{-1}$ with correlation coefficient, $r = 0.9939$, and LOD of $2.8 \times 10^{-10} \text{ mol L}^{-1}$. Four different concentrations on the calibration curve are chosen to be repeated five times to evaluate the accuracy and precision of the proposed method which is represented in (Table 3). Also the recovery, standard deviation, standard error and the confidence were calculated.

Table 3. Evaluation of the accuracy and precision of the proposed method for the determination of (TR) in urine sample.

[TR] added (M) × 10 ⁻⁶	[TR] found [a] (M) × 10 ⁻⁶	Recovery (%)	SD × 10 ⁻⁷	SE [b] × 10 ⁻⁷	CL [c] × 10 ⁻⁷
2.00	2.02	101.0	0.23	0.11	0.37
12.0	12.04	100.3	0.41	0.20	0.65
18.0	18.04	100.2	0.42	0.21	0.68
24.0	23.96	99.80	0.81	0.41	0.13

[a] mean of five determinations; [b] Standard error = SD/\sqrt{n} ; [c] CL confidence at 95% confidence level and 4 degrees of freedom ($t=2.776$).

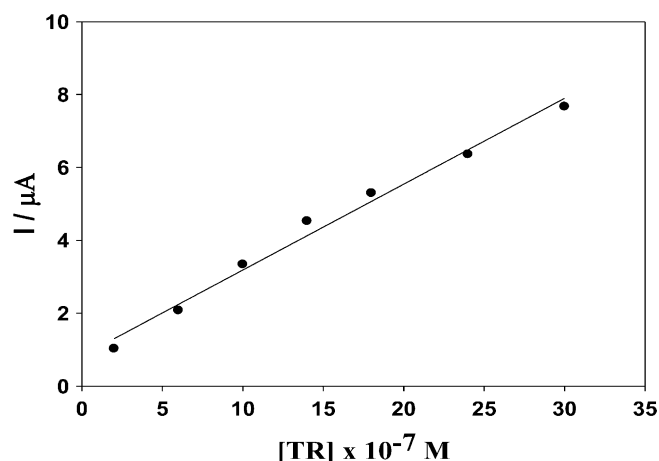


Fig. 9. Relation between TR concentration in urine and the current responses.

4 Conclusions

The binding of Trazosin (TR) to colloidal gold was studied using different analytical techniques (e.g. UV-vis spectroscopy, cyclic voltammetry, fluorescence). The nature of interaction as evidenced from fluorescence and electrochemical studies will have profound applications in biological sciences in future studies.

Owing to the unique properties of gold nanoparticles (GNP), GNMCPPE offered an improved electrochemical response for TR oxidation in neutral media. This method has advantages such as high sensitivity, very low detection limit with reasonable reproducibility, easy handling, resistance against surface fouling, and low cost. We also believe that this methodology provides an inexpensive, rapid and simple method for determining accurate TR concentrations with applications in quality control in the pharmaceutical industry. Furthermore, the proposed modified electrode was applied for the determination of TR with satisfying results, indicating that GNP will be a promising material for the measurement of TR in human urine. The developed method with the detection limits 1.2×10^{-10} M is more sensitive and selective without complexation disadvantage compared to other analytical methods.

Acknowledgements

The authors would like to express their gratitude to the *University of Cairo (Office of Vice President for Graduate Studies and Research)* for providing partial financial support through "The Young Researchers' Program". We would like to acknowledge the financial support by the *National Organization for Drug Control and Research (NODCAR, Egypt)*.

References

- [1] P. A. Abraham, C. E. Halstenson, G. R. Matzke, *Pharmacotherapy* **1985**, *5*, 285.
- [2] R. A. Graham, *Am. J. Cardiol.* **1984**, *53*, 16A.
- [3] J. J. Kyncl, *Am. J. Med.* **1986**, *80*, 12.
- [4] P. G. Fabricus, P. Weizert, U. Duzendorfer, J. M. Hannaford, C. Maurath, *Prostate* **1990**, *3*, 85.
- [5] U. Duzendorfer, *Urology* **1988**, *32*, 21.
- [6] H. Lepor, *Urology* **1995**, *45*, 406.
- [7] P. S. Sarsambi, G. K. Kapse, S. A. Raju, *Asian J. Chem.* **2002**, *14*, 545.
- [8] P. S. Sarsambi, S. A. Raju, *Asian J. Chem.* **2001**, *13*, 760.
- [9] P. S. Sarsambi, G. K. Kapse, M. Shobha, S. A. Raju, *Asian J. Chem.* **2000**, *12*, 1325.
- [10] H. H. Abdine, F. A. El-Yazbi, S. M. Blaih, R. A. Shaalan, *Spectr. Lett.* **1998**, *31*, 969.
- [11] C. Q. Jiang, M. X. Gao, J. X. He, *Anal. Chim. Acta* **2002**, *452*, 185.
- [12] A. J. Wood, P. Bolli, F. O. Simpson, *J. Clin. Pharmacol.* **1976**, *3*, 199.
- [13] Z. Hong-Yan, W. Hai-Long, Y. Li-Qun Ou, Z. Yan, N. Jin-Fang, F. Hai-Yan, Y. Ru-Qin, *Anal. Chim. Acta* **2009**, *650*, 143.
- [14] C. C. Wang, M. O. Luconi, A. N. Masi, L. Fernández, *Talanta* **2007**, *72*, 1779.
- [15] M. M. Ghoneim, M. A. El Ries, E. Hammam, A. M. Belta-gi, *Talanta* **2004**, *64*, 703.
- [16] Y. G. Yee, P. C. Rubin, P. Meffin, *J. Chromatogr.* **1979**, *172*, 313.
- [17] R. Ferretti, B. Gallinella, F. La Torre, L. Zanitti, L. Turchetto, A. Mosca, R. Cirilli, *Chromatogr. A* **2009**, *1216*, 5385.
- [18] R. C. Sonders, *Am. J. Med.* **1986**, *80*, 20.
- [19] P. A. Reece, *J. Chromatogr.* **1980**, *221*, 188.
- [20] P. Y. Cheah, K. H. Yuen, M. L. Liong, *J. Chromatogr. B* **2000**, *745*, 439.
- [21] A. P. Zavitsanos, T. Alebic-Kolbah, *J. Chromatogr. A* **1998**, *794*, 45.
- [22] M. Bakshi, T. Ojha, S. Singh, *J. Pharm. Biomed. Anal.* **2004**, *34*, 19.
- [23] V. K. Gupta, M. K. Pal, A. K. Singh, *Electrochim. Acta* **2009**, *54*, 6700.

- [24] N. F. Atta, A. Galal, F. M. Abu-Attia, S. M. Azab, *Electrochem. Soc.* **2010**, *157*, 116.
- [25] R. N. Goyal, M. Oyama, V. K. Gupta, S. P. Singh, R. A. Sharma, *Sens. Actuators B, Chem.* **2008**, *134*, 816.
- [26] V. K. Gupta, A. K. Singh, B. Gupta, *Anal. Bioanal. Chem.* **2007**, *389*, 209.
- [27] N. F. Atta, M. F. El-Kady, A. Galal, *Sens. Actuators B, Chem.* **2009**, *141*, 566.
- [28] N. F. Atta, A. Galal, R. A. Ahmed, *Bioelectrochemistry* **2011**, *80*, 132.
- [29] C. Ding, F. Zhao, R. Ren, J. M. Lin, *Talanta* **2009**, *78*, 1148.
- [30] D. Tang, R. Yuan, Y. Chai, *Anal. Chim. Acta* **2006**, *564*, 158.
- [31] M. B. González-García, C. Fernández-Sánchez, A. Costa-García, *Biosens. Bioelectron.* **2000**, *15*, 315.
- [32] M. L. Mena, P. Yáñez-Sedeño, J. M. Pingarrón, *Anal. Biochem.* **2005**, *336*, 20.
- [33] H. Huang, P. Ran, Z. Liu, *Bioelectrochemistry* **2007**, *70*, 257.
- [34] S. Upadhyay, G. R. Rao, M. K. Sharma, B. K. Bhattacharya, V. K. Rao, R. Vijayaraghavan, *Biosens. Bioelectron.* **2009**, *25*, 832.
- [35] K. Márquez, R. Ortiz, J. W. Schultze, O. P. Márquez, J. Márquez, *Electrochim. Acta* **2003**, *48*, 711.
- [36] M. Moreno, E. Rincon, J. M. Pérez, V. M. González, A. Domingo, E. Dominguez, *Biosens. Bioelectron.* **2009**, *25*, 778.
- [37] J. Wang, L. Wang, J. Di, Y. Tu, *Talanta* **2009**, *77*, 1454.
- [38] Y. Ma, J. Di, X. Yan, M. Zhao, Z. Lu, Y. Tu, *Biosens. Bioelectron.* **2009**, *24*, 1480.
- [39] Y. Wang, J. Deng, J. Di, Y. Tu, *Electrochem. Commun.* **2009**, *11*, 1034.
- [40] N. Sakai, Y. Fujiwara, M. Arai, K. Yu, T. Tatsuma, *Electroanal. Chem.* **2009**, *628*, 7.
- [41] L. Wang, W. Mao, D. Ni, J. Di, Y. Wu, Y. Tu, *Electrochem. Commun.* **2008**, *10*, 673.
- [42] J. Wang, L. Wang, J. Di, Y. Tu, *Sens. Actuators B, Chem.* **2008**, *135*, 283.
- [43] A. Bendish, P. J. Russell Jr., J. J. Fox, *J. Am. Chem. Soc.* **1954**, *76*, 6077.
- [44] V. Selvaraj, M. Alagar, I. Hamerton, *Electrochim. Acta* **2006**, *52*, 1152.
- [45] J. Zheng, X. Zhou, *Bioelectrochemistry* **2007**, *70*, 408.
- [46] T. Shimizu, T. Teranishi, S. Hasegawa, M. Miyake, *J. Phys. Chem. B* **2003**, *107*, 2719.
- [47] V. Selvaraj, M. Alagar, I. Hamerton, *Electrochim. Acta* **2006**, *52*, 1152.
- [48] J. H. Yoe, A. L. Jones, *Indust. Eng. Chem. Anal. Ed.* **1944**, *16*, 14.
- [49] P. Jop, *Ann. Chim.* **1939**, *9*, 133.
- [50] T. Pagnot, D. Barchiesi, G. Tribillion, *Appl. Phys. Lett.* **1999**, *75*, 4207.
- [51] P. V. Kamat, S. Barazzouk, S. Hotchandani, *Angew. Chem. Int. Ed. Engl.* **2002**, *41*, 2764.
- [52] E. Dulkeith, A. C. Morteani, T. Niedereichhloz, T. A. Klar, J. Feldmann, S. A. Levi, F. C. J. M. Van Veggel, D. N. Reinhoudt, M. Moller, D. I. Gittins, *Phys. Rev. Lett.* **2002**, *89*, 3002.
- [53] M. M. Ghoneima, M. A. El Ries, E. Hammama, A. M. Beltagi, *Talanta* **2004**, *64*, 703.
- [54] P. Zuman, *The Elucidation of Organic Electrode Processes*, Academic Press, New York **1969**, p. 21.
- [55] N. Yang, Q. Wan and J. Yu, *Sens. Actuators B, Chem.* **2005**, *110*, 246.
- [56] W. Qijin, Y. Nianjun, Z. Haili, Z. Xinpin, X. Bin, *Talanta* **2001**, *55*, 459.
- [57] E. Souza, G. Nascimento, N. Santana, D. Ferreira, M. Lima, E. Natividade, D. Martins, J. Lima-Filho, *Sensors* **2011**, *11*, 5616.